Article

J. Mex. Chem. Soc. **2024**, *68*(2)
Regular Issue

ISSN-e 2594-0317

Fe_3O_4@NH_2@Oxalic Acid: A Convenient Catalyst for Synthesis of Pyrrolinone Derivatives

Seyran Esmaeilzadeh, Davood Setamdideh*, Fatemeh Ghanbary

Department of Chemistry, Mahabad Branch, Islamic Azad University, Mahabad, Iran.

***Corresponding author:** Davood Setamdideh, email: d.setamdideh@iau-mahabad.ac.ir; davood.setamdideh@gmail.com

Received November 11th, 2022; Accepted May 29th, 2023.

DOI: http://dx.doi.org/10.29356/jmcs.v68i2.1910

Abstract. In this context, an amine-functionalized magnetite nanoparticle was synthesized from $FeCl_3$•$6H_2O$ and 1, 2-ethylenediamine at 110 °C in ethylene glycol within 6 hours. Then, the obtained corresponding Fe_3O_4@NH_2 was used for the preparation of Fe_3O_4@NH_2@oxalic acid as organoacid-magnetic nanoparticles under ultrasonic irradiation at 60 °C within 4 hours. Its chemical structure was characterized by FT-IR, XRD, SEM, VSM, and EDAX spectra. The Fe_3O_4@NH_2@oxalic acid nanoparticles were successfully used for the synthesis of pyrrolinones derivatives in excellent yields of the products (90-95 %) within 6-10 hours at room temperature in ethanol.
Keywords: Ethylenediamine, amino-functionalization, nano-magnetite, pyrrolinones, green chemistry.

Resumen. Se sintetizó una nanopartícula de magnetita funcionalizada con aminas a partir de $FeCl_3$•$6H_2O$ y 1,2-etilendiamina a 110 °C en etilenglicol durante 6 horas. Posteriormente, el Fe_3O_4@NH_2 que se obtuvo se utilizó para la preparación de nanopartículas magnéticas organoácidas de Fe_3O_4@NH_2@ácido oxálico por irradiación ultrasónica a 60 °C durante 4 horas. Su estructura química se caracterizó por sus espectros de FT-IR, XRD, SEM, VSM, y EDAX. Las nanopartículas de Fe_3O_4@NH_2@ácido oxálico se utilizaron existosamente para sintetizar derivados de pirrolinonas con rendimientos excelentes (90-95%), en 6-10 horas de reacción a temperatura ambiente en etanol.
Palabras clave: Etilendiamina, funcionalización amino, nanomagnetita, pirrolinonas, química verde.

Introduction

The functionalization of the magnetic nanoparticles (the F-MNPs) is crucial for chemical processes, and they have many applications in medical and biological research. Meanwhile, the amine-functionalized magnetite nanoparticles (the AF-MNPs) have received more attention because of their properties such as excellent magnetism, tunable sizes, good crystallinity, and facile dispersion in water [1-13].

The AF-MNPs and their derivatives have been used for different fields in organic chemistry such as bio-conjugated to biological molecules (proteins, nucleic acids, and peptides) [1], for cellulase immobilization to prevent wastage of cellulosic resources [2], to prepare cis-pinane [3], catalyst for Heck reaction [4], synthesis of xanthenes [5], selective separation of catecholamines in urine [6], hydrogenation and Heck reactions by Pd immobilized on the AF-MNPs [7], for attachment of polyacrylic acid [8], for the treatment of gastric, colon, and pancreatic cancers in near future [9], for the synthesis of carbamates [10], for degradation of the methyl orange and *p*-nitrophenol reduction in aqueous media [11], enhanced photocytotoxicity [12], and removal of carmoisine dye from aqueous solutions [13].

J. Mex. Chem. Soc. **2024**, *68*(2)
Regular Issue

ISSN-e 2594-0317

On the other hand, pyrrolin-2-one skeleton has biological activity in some synthetic drugs and natural products, for example: *Cotinine* [14], *Doxapram hydrochloride* [15], *Ethosuximide* [16], *Rolipram* [17], *Lactacystin* [18], *Salinosporamide* [19], *(−)-Azaspirene* [20] *and Pesticides* [21] (Scheme 1).

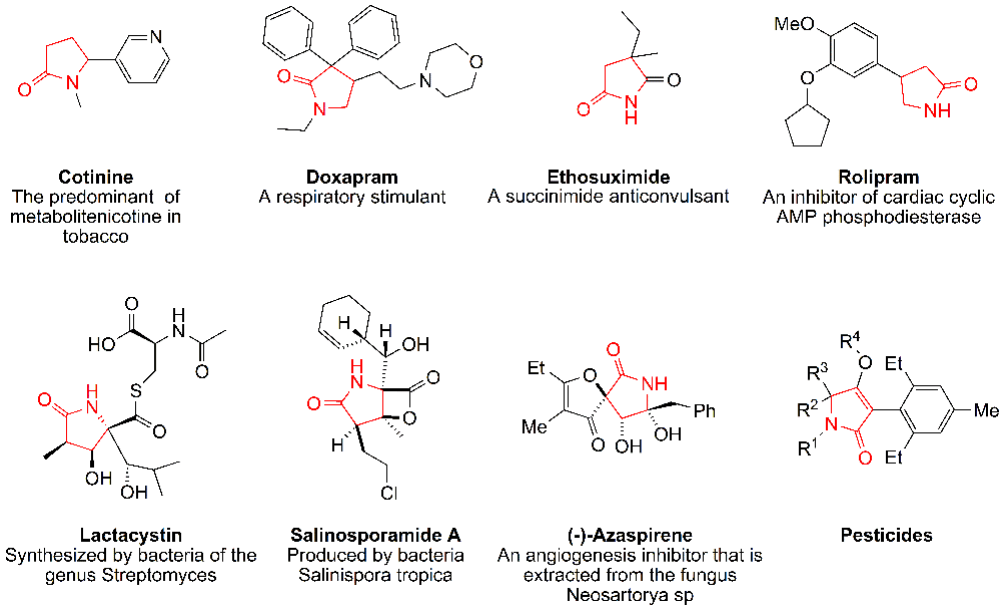

Scheme 1. The chemical structure of some natural products and drugs with pyrrolinone moiety.

Some procedures have been reported for the synthesis of pyrrolin-2-ones [22-27]. However, a coupling of arylamines and aromatic aldehydes with acetylenedicarboxylates is an important synthetic method for the synthesis of this class of compounds. This method has been studied by several protocols such as using of nano-TiO_2 [28], in water as a green solvent [29], by *p*-toluensulfonic acid [30], under ultrasound irradiation [31], or microwave irradiation [32], by ionic liquids [33], in the presence of nano-magnetic particles [34], and AmberChrom as a polymer catalyst [35]. For improving the obtained result as a part of the synthetic project we turned attention to the synthesis of a more stable and convenient catalyst for this procedure. Thus, we decided to link oxalic acid on magnetite nanoparticles by a covalent bond. Our survey showed using of amine-functionalized magnetite nanoparticles (the AF-MNPs) is a good approach for this subject. Thus, pyrrolin-2-ones were synthesized by a new methodology from aldehydes, anilines and dimethyl acetylenedicarboxylate by Fe_3O_4@NH_2@oxalic acid as a reusable nano-magnetic catalyst at room temperature (Scheme 2).

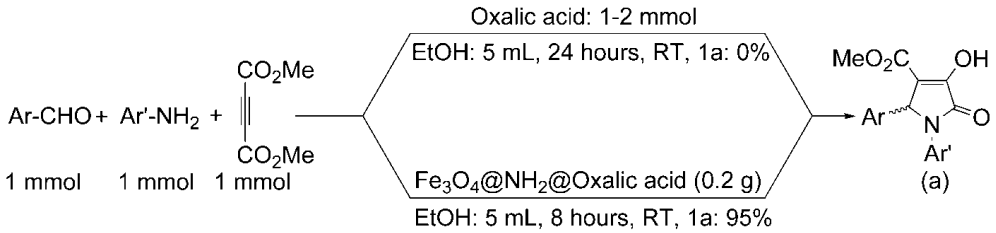

1a: Ar(Ph)Ar'(Ph)(8 h, 95%); **2a**: Ar(Ph)Ar'(4-MeOPh)(6 h, 90%); **3a**: Ar(3-ClPh)Ar'(4-MeOPh)(6 h, 95%); **4a**: Ar(4-BrPh)Ar'(4-BrPh)(10 h, 93%); **5a**: Ar(3-NO_2Ph)Ar'(4-BrPh)(10 h, 91%); **6a**: Ar(Ph)Ar'(4-BrPh)(10 h, 94%); **7a**: Ar(2-ClPh)Ar'(4-MeOPh)(6 h, 90%); **8a**: Ar(2-MeOPh)Ar'(4-MePh)(8 h, 92%)

Scheme 2. The synthesis of 1,5-diaryl-3-hydroxy-4-methoxycarbonyl-3-pyrrolin-2-ones by Fe_3O_4@NH_2@oxalic acid as a catalyst.

J. Mex. Chem. Soc. **2024**, *68*(2)
Regular Issue

ISSN-e 2594-0317

Experimental

Materials

All reagents were purchased from Sigma-Aldrich Company. FT-IR spectra were recorded on a Bruker spectrometer. XRD patterns were recorded using a Holland Philips (model: PW1730) (radiation, λ= 0.154056 nm, CuK), Step size 0.05°, time per step 1 second (2θ=5°-80°). SEM images were performed on a Model FESEM: TESCAN company (model: MIRA III) manufactured by Czech. EDX (Energy Dispersive X-Ray Analysis) was taken by FESEM: model: MIRA II from TESCAN company manufactured by Czech (Detector: SAMX, France). VSM analysis was taken by model MDKB manufactured by Kavir Kashan Magnet Company (Iran). TGA analysis was recorded by Model Q600; TA company manufactured by the USA. IR and ^{1}H NMR spectra were recorded on PerkinElmer FT-IR RXI and 300 MHz Bruker spectrometers, respectively. Pyrrolinone derivatives were characterized by their ^{1}H-NMR, FT-IR spectra. All yields referred to isolated pure products. TLC was applied for reaction monitoring over silica gel 60 F_{254} aluminum sheet.

Synthesis of Fe_3O_4@NH_2 nanoparticles

The magnetic amine-functionalized nanoparticles (Fe_3O_4@NH_2) were prepared *via* solvothermal reaction with major modification [1]. $FeCl_3.6H_2O$ (1.5 gr), 1, 2-ethylenediamine (3 g), and sodium acetate anhydrous (12 g) were dissolved in ethylene glycol (45 mL) *via* vigorous mechanical stirring. Then, the reaction was heated at 110°C for 6 hours under the Ar atmosphere. The obtained magnetic nanoparticles were isolated by a powerful magnet, and washed with distilled H_2O, and EtOH several times. Then, the product was dried at 60 °C for 2 hours.

Preparation of Fe_3O_4@NH_2@Oxalic acid nanoparticles

Fe_3O_4@NH_2 nanoparticles (0.25 g) were dispersed in ethanol (15 mL) by ultrasonic bath for 30 minutes. Then, a solution of oxalic acid (0.4 g) in ethanol-water (20mL/10mL) was prepared and was charged in the above solution. The obtained mixture was irradiated by ultrasonic irradiation for 4 hours at 60 °C under the Ar atmosphere. The obtained magnetic nanoparticles (i.e Fe_3O_4@NH_2@Oxalic acid) were isolated by a powerful magnet, washed with ethanol, and distilled water several times to remove all organic impurities. Then, the product was dried at 60 °C for 2 hours.

The synthesis of 1,5-diphenyl-3-hydroxy-4-methoxycarbonyl-3-pyrrolin-2-one (1a) by Fe_3O_4@NH_2@oxalic acid; A typical procedure

A mixture of benzaldehyde (0.106 g, 1 mmol), aniline (0.093 g, 1 mmol), and Fe_3O_4@NH_2@oxalic acid (0.2 g) in 5 mL of ethanol was prepared in a round-bottomed flask (25 mL) equipped with a magnetic stirrer and was strongly stirred at room temperature for 40 min. Then to the mixture dimethyl acetylenedicarboxylate (0.14 gr, 1 mmol) was added. The reaction was completed within 8 hours. The reaction was monitored over silica gel 60 F_{254} aluminum sheet (eluent: ethyl acetate/*n*-hexane: 1/1). The catalyst was separated by using a strong magnet. The separated catalyst was washed with acetone and ethanol two times then dried in an oven (50 °C) and reused for further reactions. The solvent has been evaporated by a rotary instrument and further residue was recrystallized from methanol. The white solid achieved an excellent yield of 0.295 g (95 %) with a melting point of 182–183 °C [30]. The product was characterized by ^{1}H-NMR, ^{13}C-NMR, FT-IR and C, H, N elemental analysis.

FT- IR (KBr)(cm^{-1}): 3260 (OH), 2958, 1702 (C=O), 1680 (C=O), 1498, 1382, 1232, 1002; ^{1}H NMR ($CDCl_3$): δ 3.60 (s, 3H, CH_3), 6.10 (s, 1H, CH), 7.07–7.62 (m, 10 H, Ar and br s, 1H, OH); ^{13}C NMR ($CDCl_3$): δ 50.55, 61.05, 112.35, 122.96, 125.80, 128.13, 128.38, 128.73, 129.13, 136.74, 137.00, 153.14, 162.96 (C=O), 164.49 (C=O). Anal. Calcd for $C_{18}H_{15}NO_4$: C, 69.89; H, 4.89; N, 4.53. Found: C, 69.92; H, 4.81; N, 4.48.

Results and discussion

A literature survey showed that the preparation of the AF-MNPs by direct coupling of amino agents to magnetite nanoparticles has been carried out by different chemical procedures. The chemical conditions for these methods have been summarized in table 1 for more consideration.

J. Mex. Chem. Soc. **2024**, *68*(2)
Regular Issue

ISSN-e 2594-0317

Table 1. Synthesis of the AF-MNPs by different protocols.

Entry	Magnetite source	Amino agent	Steps	Size, nm
1[1-3, 7-8, 40, 44-46, 48, 50, 52-53]	$FeCl_3$•$6H_2O$	1,6-hexadiamine	1	1.95-200
2[5]	$FeCl_3$•$6H_2O$ & $FeCl_2$•$4H_2O$	1,6-hexadiamine	1	20
3[6, 38, 49]	$FeCl_3$•$6H_2O$ & $FeCl_2$•$4H_2O$	$H_2N(CH_2)_3Si(OCH_3)_3$	2	13-150
4[36a]	$FeCl_3$•$6H_2O$	$H_2N(CH_2)_3Si(OCH_3)_3$	2	250
5[36]	$FeCl_3$•$6H_2O$ & $FeSO_4$•$7H_2O$	$H_2N(CH_2)_3Si(OCH_3)_3$	2	10
6[42, 45]	$Fe(NO_3)_3$•$9H_2O$	$H_2N(CH_2)_3Si(OCH_3)_3$	2	20-40
7[4, 39, 41]	$FeCl_3$•$6H_2O$	triethylenetetramine	1	70-100
8[37]	$FeCl_3$•$6H_2O$ & $FeCl_2$•$4H_2O$	$(CH_3O)_3Si(CH_2)_3NH(CH_2)_2NH(CH_2)_2NH_2$	2	20-100
9[43]	$FeCl_3.6H_2O$	poly(propyleneglycol)bis (2-aminopropyl ether)	1	20
10[47]	$FeCl_3$•$6H_2O$	2,2'-(ethylenedioxy)-bis-(ethylamine)	1	6
11[51]	$FeCl_3$•$6H_2O$	2-aminoterephthalic acid	2	4
12[6]	$FeCl_3$•$6H_2O$ & $FeSO_4$•$7H_2O$	$H_2N(CH_2)_3Si(OEt)_3$	2	none

In continuous of these procedures (table 1), Fe_3O_4@NH_2 was synthesized by a new protocol. The magnetite nanoparticles were prepared from $FeCl_3$•$6H_2O$. Also, 1, 2-ethylenediamine was used as an amino agent. As shown in table 2, some experiments were carried out for optimizing the best ratio of the reagents, temperature, and reaction time. All reactions were performed by a one-pot reaction of $FeCl_3$•$6H_2O$ and 1, 2-ethylenediamine in the ratio (1:10) in ethylene glycol at different temperatures & times under an inert atmosphere.

J. Mex. Chem. Soc. **2024**, *68*(2)
Regular Issue

ISSN-e 2594-0317

Table 2. Optimization reaction conditions for the synthesis of Fe_3O_4@NH_2 (product) from $FeCl_3$•$6H_2O$ (A), 1, 2-ethylenediamine (B), and sodium acetate anhydrous (C) in ethylene glycol (45 mL).

Entry	A/g	B/g	C/g	*θ*/° C	*t*/*h*	Product
1	1.5	2	3	150-190	3 and 6	impure
2	1.5	3	6	200	3 and 6	impure
3	1.5	2	12	200	6	impure
4	1.5	3	6	110	3	poor quality
5	1.5	3	12	110	6	good quality
6	1.5	3	6	110	12	poor quality

The quality of the obtained AF-MNPs was determined by comparing FT-IR spectra as shown in Fig. 1**(a-c)**. In Fig. 1**(a)**, the band at 645 cm^{-1} assigned to the impurity some amount of maghemite [36b] when the reactions were carried out at 200 °C (table 2, entry 2-3). The same results were achieved at 150-190 °C (table 2, entry 1). Due to the absorbance bands at 3428 cm^{-1} (NH stretching vibration) and 2934 and 2862 cm^{-1} (asymmetric stretching vibration and symmetric stretching vibration of CH_2), 1, 2-ethylenediamine was coated better at 110 °C within 6 hours (Fig. 1**(c)**) (Table 2, entry 5), while the coating was reduced in fewer time of reaction (3 hours, Fig. 1**(b)**) (Table 2, entry 4).

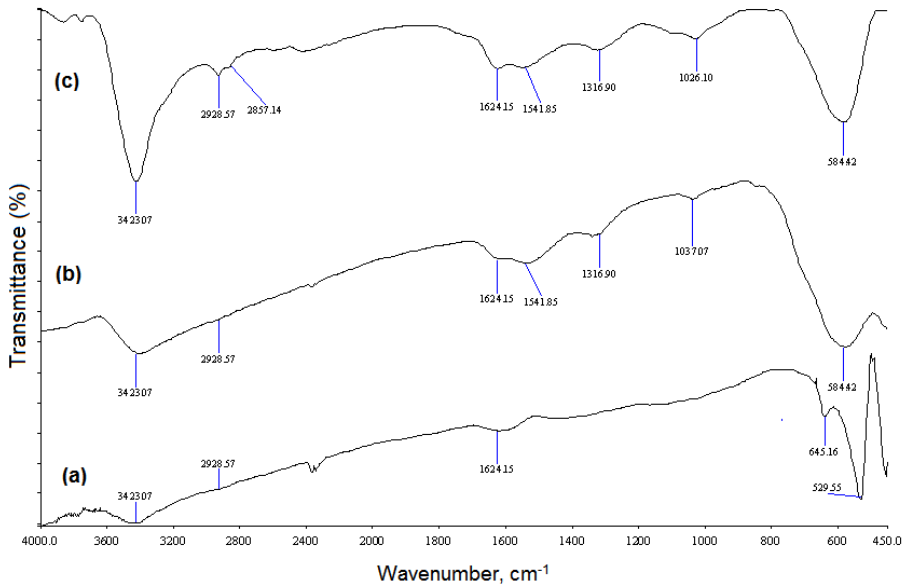

Fig. 1. (a) FT-IR spectrum of synthesized of Fe_3O_4-CH_2CH_2-NH_2 at 200 °C within 6 hours (Table 2, entry 3). **(b)** FT-IR spectrum of synthesized of Fe_3O_4-CH_2CH_2-NH_2 at 110 °C within 3 hours (Table 2, entry 4). **(c)** FT-IR spectrum of synthesized of Fe_3O_4-CH_2CH_2-NH_2 at 110 °C within 6 hours (Table 2, entry 5).

Thus, the results (Table 2, entry 5) showed that a one-pot reaction of $FeCl_3$•$6H_2O$ and 1, 2-ethylenediamine in the ratio (1:10) at 110 °C within 6 hours in ethylene glycol gave the best quality and quantity

J. Mex. Chem. Soc. **2024**, *68*(2)
Regular Issue

ISSN-e 2594-0317

of Fe_3O_4-CH_2CH_2-NH_2 (Fe_3O_4@NH_2) as shown in Scheme 1. The chemical structure of Fe_3O_4@NH_2 was characterized by FT-IR and VSM spectra.

A one-pot reaction of $FeCl_3.6H_2O$ and 1, 2-ethylenediamine in the ratio (1:10) at 110 °C within 6 hours in ethylene glycol gave the best quality and quantity of Fe_3O_4-CH_2CH_2-NH_2 (Fe_3O_4@NH_2) as shown in Scheme 3.

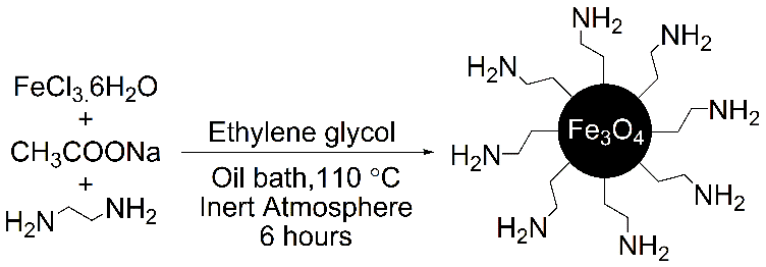

Scheme 3. The synthesis of Fe_3O_4@NH_2 nanoparticles.

Then, oxalic acid as an organic acid was linked to surface of Fe_3O_4@NH_2 nanoparticles. The best reaction conditions were obtained by performing some reactions in different conditions as shown in Table 3.

Table 3. Optimization reaction conditions for the synthesis of Fe_3O_4@NH_2@oxalic acid (product) from Fe_3O_4@NH_2 (1 g) under the Ar atmosphere.

Entry	$m_{\text{oxalic acid}}$ / g	Conditions	θ / °C	t / h	Product[1]
1	0.4	-	RT	2 or 4	no
2	0.4	ultrasonic	RT	2 or 4	no
3	0.8	ultrasonic	40	2 or 4	no
4	1.2	ultrasonic	40	2 or 4	no
5	1.2	ultrasonic	60	2	no
6	1.2	ultrasonic	60	4	yes
7	1.2	-	60	4	no
8[2]	1.6	ultrasonic	60	4	yes
9[2]	1.2	ultrasonic	60	8	yes

[1]The formation of the product (Fe_3O_4@NH_2@oxalic acid) was characterized by FT-IR spectrum.
[2]The obtained results from entries 8 and 9 are similar to entry 6. These results showed that more amounts of oxalic acid and more reaction time for the preparation of the product are not required.

The results showed (Table 3, entry 6) that oxalic acid can be linked by using ultrasonic irradiation at 60 °C within 4 hours under the Ar atmosphere. Thus, the Fe_3O_4-CH_2CH_2NH-CO-CO_2H (Fe_3O_4@NH_2@oxalic acid) nanoparticles were successfully synthesized, as shown in Scheme 4. The chemical structure of the Fe_3O_4@NH_2@oxalic acid was characterized by FT-IR, XRD, SEM, VSM, and EDAX spectra.

J. Mex. Chem. Soc. **2024**, *68*(2)
Regular Issue

ISSN-e 2594-0317

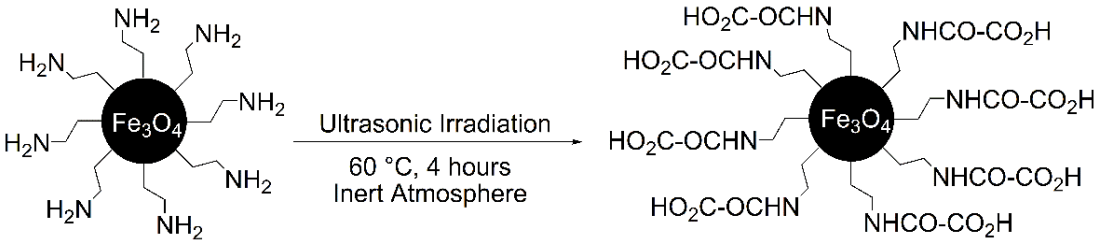

Scheme 4. The synthesis of Fe_3O_4@NH_2@oxalic acid nanoparticles from Fe_3O_4@NH_2 nanoparticles under ultrasonic irradiations.

The FT-IR spectrum of Fe_3O_4-CH_2CH_2-NH_2 (Fe_3O_4@NH_2) is shown in Fig. 2**(a)**. The band at 3428 cm^{-1} was assigned to NH stretching vibration which was combined with OH stretching vibration of the absorbed water on Fe_3O_4. The bands at 2934 cm^{-1} and 2862 cm^{-1} were assigned to asymmetric stretching vibration and symmetric stretching vibration of CH_2. The band at 1626 cm^{-1} was assigned to OH bending vibration of the absorbed water on Fe_3O_4. The band at 1547 cm^{-1} was assigned to NH bending vibration. The band at 1316 cm^{-1} was assigned to C–C stretching of vibration. The band at 1023 cm^{-1} was assigned to C–N stretching vibration and the band at 583 cm^{-1} was assigned to the Fe–O bending vibration [34b].

The FT-IR spectrum of Fe_3O_4-CH_2CH_2NH-CO-CO_2H (Fe_3O_4@NH_2@oxalic acid) has been shown in Fig. 2**(b)**. The band at 3394 cm^{-1} was assigned to OH stretching vibration of the COOH group. The band at 1684 cm^{-1} and 1673 cm^{-1} were assigned to C=O bond stretching vibrations of the COOH and CO-NH groups, respectively. The band at 1397 cm^{-1} was assigned to OH bending vibration of the COOH group. The band at 1267 cm^{-1} was assigned to C–O stretching vibration. The band at 1037 cm^{-1} was assigned to C–N stretching vibration. The band at 787 cm^{-1} was assigned to OH bending vibration of the COOH group, and 567 cm^{-1} was assigned to the Fe–O bending vibration.

A comparison of the FT-IR spectra of Fe_3O_4@NH_2 in Fig. 2**(a)** and Fe_3O_4@NH_2@oxalic acid in Fig. 2**(b)** shows that a band at 1626 cm^{-1} in Fig. 1**(a)** does not appear in the FT-IR spectrum of Fe_3O_4@NH_2@oxalic acid Fig. 2**(b)**. Because this band was replaced by a doublet band at 1684 cm^{-1} (acidic C=O) and 1673 cm^{-1} (amide C=O). This result that was indicated the successful attachment of oxalic acid to Fe_3O_4@NH_2 nanoparticles.

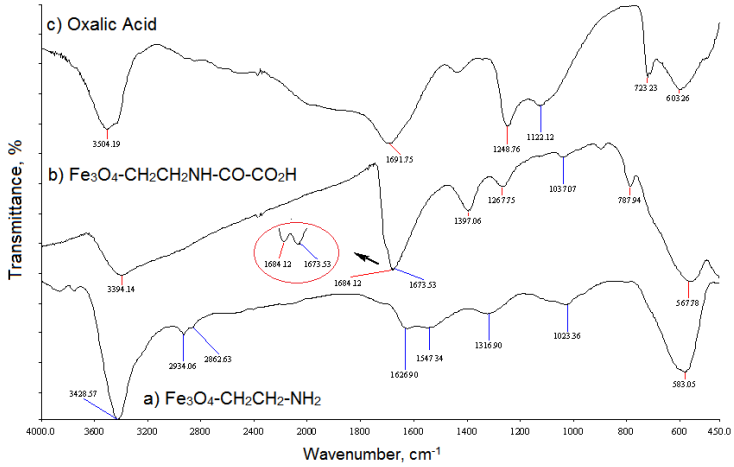

Fig. 2. The FT-IR spectra of **(a)** Fe_3O_4-CH_2CH_2-NH_2 (Fe_3O_4@NH_2), **(b)** Fe_3O_4-CH_2CH_2NH-CO-CO_2H, (Fe_3O_4@NH_2@oxalic acid) **(c)** oxalic acid.

J. Mex. Chem. Soc. **2024**, *68*(2)
Regular Issue

ISSN-e 2594-0317

The VSM spectrum was used to evaluate the magnetic measurement of magnetite nanoparticles at room temperature as shown in Fig. 3**(a)**. Due to the lack of magnetic remanence and coercivity, the room-temperature magnetization curve of the Fe_3O_4@NH_2 and Fe_3O_4@NH_2@oxalic acid nanoparticles suggests a paramagnetic state of the nanoparticles. The magnetization curves indicate the saturation magnetization of Fe_3O_4@NH_2@oxalic acid and Fe_3O_4@NH_2 nanoparticles, which were diminished to 10.50 emu/g from 12.90 emu/g. These results are significantly smaller than reported values for bulk Fe_3O_4 (92 emu/g and 100 emu/g) [54]. In the Fe_3O_4@NH_2 and Fe_3O_4@NH_2@oxalic acid adsorbed water, amine agent, and oxalic acid reduce the measured magnetic strength because magnetic nanoparticles are diluted with diamagnetic physically.

The SEM images of nano-Fe_3O_4@NH_2@oxalic acid (Fig. 3**(b)**) show the presence of spheric nanoparticles with 81 nm of average diameter.

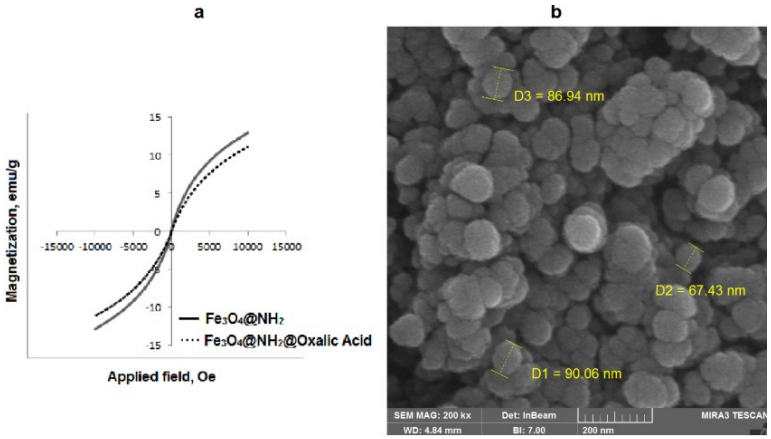

Fig 3. a) The room-temperature magnetization curve of the Fe_3O_4@NH_2 and Fe_3O_4@NH_2@oxalic acid nanoparticles. b) The SEM spectra of Fe_3O_4@NH_2@oxalic acid.

The XRD patterns of the Fe_3O_4@NH_2@oxalic acid nanoparticles are presented in Fig. 4. The peak positions are indexed as (111), (220), (331), (400), (422), (511), (440), (620), (533) and (444) in the 2θ range of 20–80°. These results reveal the existence of a Fe_3O_4 core in the Fe_3O_4@NH_2@oxalic acid which is in good agreement with the literature [54-55]. Fig. 5 shows EDAX analysis of Fe_3O_4@NH_2@oxalic acid nanoparticles. The sample peaks are observed for carbon, oxygen, iron, and nitrogen. It reveals that carbon was from 1, 2-ethylenediamine and oxalic acid, oxygen from oxalic acid and Fe_3O_4, iron from Fe_3O_4, and nitrogen from 1, 2-ethylenediamine. These results shows that surface of Fe_3O_4 was coated more than 93 % by organic materials (1, 2-ethylenediamine, and oxalic acid).

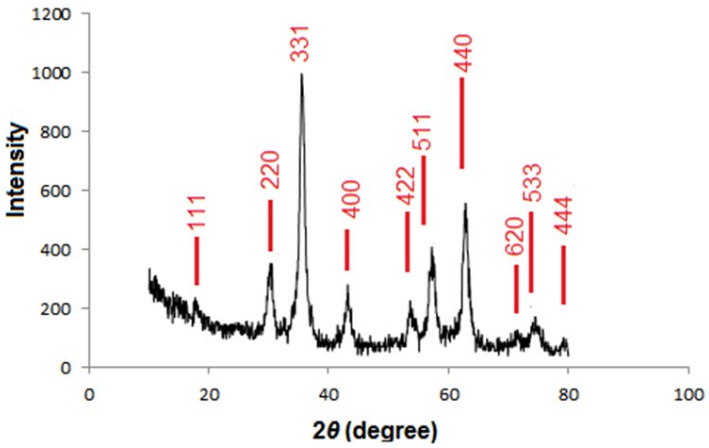

Fig 4. The XRD patterns of Fe_3O_4@NH_2@oxalic acid nanoparticles.

J. Mex. Chem. Soc. **2024**, *68*(2)
Regular Issue

ISSN-e 2594-0317

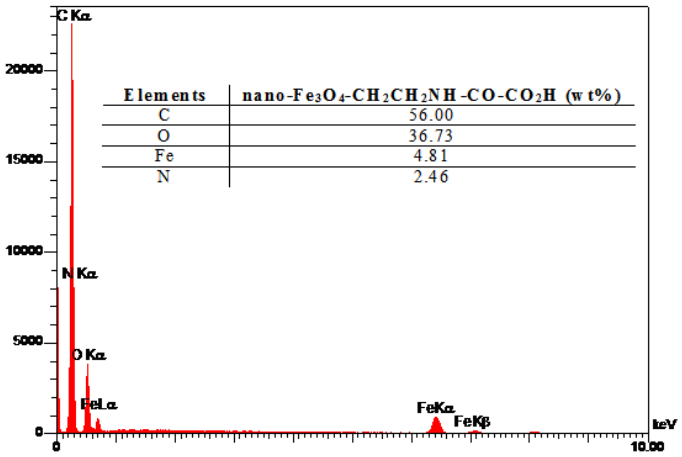

Fig 5. EDAX analysis of Fe_3O_4@NH_2@oxalic acid nanoparticles.

The synthesized Fe_3O_4@NH_2@oxalic acid nanoparticles were used for the synthesis of pyrrolin-2-one derivatives after optimum reaction conditions as shown in Table 4. It was best to combine benzaldehyde (1 mmol), aniline (1 mmol), and 0.2 g Fe_3O_4@NH_2@oxalic acid nanoparticles as the catalyst in ethanol. The reaction was completed after 8 hours to give the corresponding pyrrolin-2-ones in 95 % yields as shown in Scheme 2.

Table 4. Optimization reaction conditions for the synthesis of 1,5-diphenyl-3-hydroxy-4-methoxycarbonyl-3-pyrrolin-2-one in the presence of Fe3O4@NH2@oxalic acid nanoparticles as catalyst at room temperature.[a]

Entry	Catalyst	Amounts (g)	Solvent	*t*/h	Yields, %[b]
1	Fe_3O_4@NH_2@oxalic acid	0.1	EtOH	12	35
2	Fe_3O_4@NH_2@oxalic acid	0.15	EtOH	12	60
3	Fe_3O_4@NH_2@oxalic acid	0.2	EtOH	8	95
4	Fe_3O_4@NH_2@oxalic acid	0.5	EtOH	6	93
5	Fe_3O_4@NH_2@oxalic acid	1	EtOH	6	90
6	Fe_3O_4@NH_2@oxalic acid	0.2	MeOH	2	90
7	Fe_3O_4@NH_2@oxalic acid	0.2	EtOAc	24	75
8	Fe_3O_4@NH_2@oxalic acid	0.2	H_2O	24	0
9	Fe_3O_4@NH_2@oxalic acid	0.2	THF	24	47

[a]benzaldehye (1 mmol), aniline (1 mmol), DAMD (1 mmol). [b]The yields were referred to as isolated products.

For more proofing, the reaction of a variety of anilines and aromatic aldehydes was performed under optimized reaction conditions. All the reactions were completed within 6-10 hours in the excellent yields of pure products (1-8a) (90-95 %) as shown in scheme 2. All products were characterized by FT-IR, ^{1}H-NMR, ^{13}C-NMR and C. H, N elemental analysis. In the ^{1}H-NMR spectrum, the chemical shifts of the CH group in the

J. Mex. Chem. Soc. **2024**, *68*(2)
Regular Issue

ISSN-e 2594-0317

heterocyclic ring appear around 5.62-6.41 ppm, as a single signal. In the FT-IR spectrum, the C=O stretching frequency of the products appears around 1675-1693 cm^{-1}. The melting points of the products were measured and compared with the literature [30-35].

Due to the chemical structure of Fe_3O_4@NH_2@oxalic acid, CO_2H groups can provide an acidic surface with good polarity. All moieties in this reaction are polar. Thus, they can react and condensate more easily on Fe_3O_4@NH_2@oxalic acid surface by dipolar-dipolar interactions. Fe_3O_4@NH_2@oxalic acid nanoparticles activate the aldehyde functional group for reaction with aniline. Thus, an imine as an intermediate (step (I), Scheme 3) is produced. Then, the obtained H_2O molecules from this condensation reaction, react with DMAD and produce a 1,3-dipolar intermediate (step (II), Scheme 3) [30], which would undergo the addition to the imine (step (III & IV), Scheme 3). Then, an intramolecular attack of the amino group on one of the esters results in the formation of the five-membered ring as pyrrolin-2-one skeleton (a, step (V), Scheme 3).

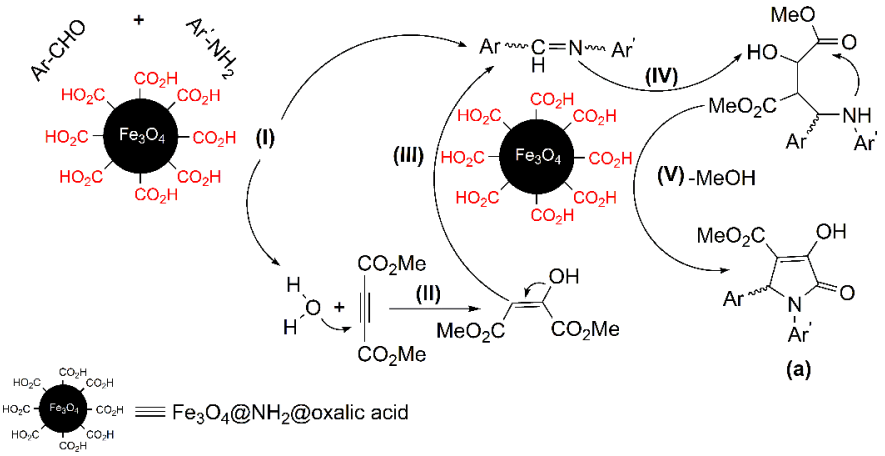

Scheme 3. The schematic and the tentatively proposed mechanism for the synthesis of pyrrolin-2-one derivatives by Fe_3O_4@NH_2@oxalic acid as catalyst.

Table 5. Comparison of synthesis of 1,5-diphenyl-3-hydroxy-4-methoxycarbonyl-3-pyrrolin-2-one by Fe3O4@NH2@oxalic acid with the different protocols.

Entry	Protocol	Yield	t/*h*	Green Profile	Availability	Reusable Catalyst	Reference
1	Fe_3O_4@NH_2@oxalic acid/EtOH/RT	95	8	yes	yes	yes	current
2	EtOH/H_2O/RT	87	15	yes	yes	no	29
3	*P*-TsOH/EtOH/RT	62	48	no	yes	no	30
4	Citric Acid/US/ EtOH/RT	90	0.3	yes	no	no	31
5	*P*-TsOH/MW/EtOH/RT	96	0.1	no	no	no	32
6	TiO_2 admicelle/H_2O/RT	75	18	yes	no	no	28
7	[bmim]BF_4/PEG-400/RT	89	1	yes	no	yes	33a
8	MW/[BBSI]Cl/Ethylene glycol/RT	90	0.1	yes	no	yes	33b

J. Mex. Chem. Soc. **2024**, *68*(2)
Regular Issue

ISSN-e 2594-0317

9	[BBSI]Cl/ball milling/RT	90	0.5	yes	no	yes	33c
10	[BBSI]HSO_4/ball milling/RT	87	0.4	yes	no	yes	33c
11	Fe_3O_4@SiO_2@Propyl–ANDSA/EtOH/RT	87	8	yes	no	yes	34
12	Fe_3O_4@PEG-400@oxalic acid/MeOH/RT	90	24	yes	no	yes	35
13	LEDs/Rose Benga /CH_3CN-H_2O	94	0.8	yes	no	yes	56
14	AmberChrom/brine/ EtOH/RT	95	6	yes	yes	yes	35

The reusability of Fe_3O_4@NH_2@oxalic acid catalyst was examined. The recycled catalyst can be used three more times. For example, the second and third rounds yields of the product (Scheme 2, 1a) were 92 % and 93 % respectively. For more consideration, the efficiency of Fe_3O_4@NH_2@oxalic acid nano-magnetic catalyst for the synthesis of 1,5-diphenyl-3-hydroxy-4-methoxycarbonyl-3-pyrrolin-2-one (Sheme 2, 1a) has been compared with other reported protocols as shown in Table 5. The comparison shows Fe_3O_4@NH_2@oxalic acid catalyst has a good potential for the synthesis of pyrrolin-2-one derivatives.

Conclusions

In this research, the Fe_3O_4@NH_2 nanoparticle was synthesized from $FeCl_3$•$6H_2O$ and 1, 2-ethylenediamine. Then, Fe_3O_4@NH_2@oxalic acid as an organoacid-magnetic nanoparticle was synthesized by coupling of Fe_3O_4@NH_2 nanoparticle and oxalic acid under ultrasonic irradiations. Also, the nano-Fe_3O_4@NH_2@oxalic acid was used for preparation of a variety of pyrrolin-2-ones. The reactions were performed in ethanol in the excellent of yields at room temperature. The recovered and regenerated catalyst can be useful for reaction with loss of activity. Thus, easy work-up, mild reaction conditions, recyclability, recovery, non-toxicity, economically affordable, and high efficiency are valuable characteristics that make this new method noteworthy.

Acknowledgements

The authors gratefully acknowledge the financial support of this work by the Research Council of the Islamic Azad University, Mahabad Branch, Mahabad, Iran. DOI:

References

1. Wang, L.; Bao, J.; Wang, L.; Zhang, F.; Li, Y. *Chem. Eur. J.* **2012**, *12*, 6341- 6343. DOI: https://doi.org/10.1002/chem.200501334.
2. Hana, J.; Wang, L.; Wang, Y.; Dong, J.; Tang, X.; Ni, L.; Wang, L. *Biochem. Eng. J.* **2018**, *130*, 90-98. DOI: https://doi.org/10.1016/j.bej.2017.11.008.

J. Mex. Chem. Soc. **2024**, *68*(2)
Regular Issue

ISSN-e 2594-0317

3. Liua, Y.; Lib, L.; Liub, S.; Xiea, C.; Yub, S. *J. Mol. Catal. A. Chem.* **2016**, *424*, 269-275. DOI: https://doi.org/10.1016/j.molcata.2016.09.007.
4. Ma, M.; Zhang, Q.; Yin, D.; Dou, J.; Zhang, H.; Xu, H. *Catal. Commun.* **2012**, *17*, 168-172. DOI: https://doi.org/10.1016/j.catcom.2011.10.015.
5. Naeimi, H.; Ansarian, Z. *J. Taiwan Inst. Chem. Eng.* **2018**, *85*, 265-272. DOI: https://doi.org/10.1016/j.jtice.2018.01.047.
6. Han, Q.; Wu, X.; Cao, Y.; Zhang, H.; Zhao, Y.; Kang, X.; Zhu, H. *Separations* **2021**, *8*, 196 https://doi.org/10.3390/separations8110196.
7. Zhang, F.; Jin, J.; Zhong, X.; Li, S.; Niu, J.; Li, R.; Ma, J. *Green Chem.* **2011**, *13*, 1238-1243. DOI: https://doi.org/10.1039/C0GC00854K.
8. Xu, Y. Y.; Zhou, M.; Geng, H. J.; Hao, J. J.; Ou, Q. Q. *Appl. Surf. Sci.* **2012**, *258*, 3897-3902. DOI: https://doi.org/10.1016/j.apsusc.2011.12.054
9. Wang, X.; Almoallim, H. S.; Cui, Q.; Alharbi, S. A.; Yang, H. *Int. J. Biol. Macromol* **2021**, *171*, 198-207. DOI: https://doi.org/10.1016/j.ijbiomac.2020.12.037.
10. Sharma, K.; Dutta, S.; Sharma, S. *Dalton Trans.* **2015**, *44*, 1303-1316. DOI: https://doi.org/10.1039/C4DT03236E.
11. Snoussi, Y.; Bastide, S.; Abderrabba, M.; Chehimi, M. M. *Ultrason. Sonochem.* **2018**, *41*, 551-561. DOI: https://doi.org/10.1016/j.ultsonch.2017.10.021.
12. Zhang, Z.; Zhu, Y.; Dai, R.; Zhang, Y.; Wang, H.; Li, J. *Photodiagnosis Photodyn. Ther.* **2018**, *23*, 50-54. DOI: https://doi.org/10.1016/j.pdpdt.2018.06.002.
13. Gemeay, A. H.; Keshta, B. E.; El-Sharkawy, R. G.; Zaki, A. B. *Environ. Sci. Pollut. Res.* **2020**, *27*, 32341-32358. DOI: https://doi.org/10.1007/s11356-019-06530-y.
14. Dwoskin, P.; Teng, L.; Buxton, S. T.; Crooks, P. A. *J. Pharmacol. Exp. Ther*. **1999**, *288*, 905-911. DOI:https://jpet.aspetjournals.org/content/288/3/905.short.
15. Singh, P.; Dimitriou, V.; Mahajan, R. P.; Crossley, A. W. *Br. J. Anaesth*. **1993**, *71*, 685-688. DOI: https://doi.org/10.1093/bja/71.5.685.
16. Patsalos, P. N. *Epilepsia* **2005**, *46*, 140-148. DOI: https://doi.org/10.1111/j.1528-1167.2005.00326.x.
17. Lampe, J. W.; Chou, Y.; Hanna, R. G.; Di Meo, S. V.; Erhardt, P. W.; Hagedorn, A. A.; Ingebretsen, W. R.; Cantor, E. *J. Med. Chem.* **1993**, *36*, 1041-1047. DOI: https://doi.org/10.1021/jm00060a012.
18. Omura, S.; Fujimoto, T.; Otoguro, K.; Matsuzaki, K.; Moriguchi, R.; Tanaka, H.; Sasaki, Y. *J. Antibiot.* **1991**, *44*, 113-116. DOI: https://doi.org/10.7164/antibiotics.44.113.
19. Feling, R. H.; Buchanan, G. O.; Mincer, T. J.; Kauffman, C. A.; Jensen, P. R.; Fenical, W. *Angew. Chem. Int. Ed.* **2003**, *42*, 355-357. DOI: https://doi.org/10.1002/anie.200390115.
20. Asami, Y.; Kakeya, H.; Onose, R.; Yoshida, A.; Matsuzaki, H.; Osada, H. *Org. Lett.* **2002**, *4*, 2845-2848. DOI: https://doi.org/10.1021/ol020104+.
21. Fischer, R.; Lehr, S.; Drewes, M. W.; Feucht, D.; Malsam, O.; Bojack, G.; Arnold, C.; Auler, T.; Hills, M.; Kehne, H. German Patent DE 102004053191 2006.
22. Franco, M. S. F.; Casagrande, G. A.; Raminelli, C.; Moura, S.; Rossatto, M.; Quina, F. H.; Pereira, C. M. P.; Flores, A. F. C.; Pizzuti, L. *Synth. Commun.* **2015**, *45*, 692-701. DOI: https://doi.org/10.1080/00397911.2014.978504.
23. Andana, M.; Hashimoto, S. I. Tetrahedron *Lett.* **1998**, *39*, 79-82. DOI: https://doi.org/10.1016/S0040-4039(97)10493-2.
24. Choi, D. R.; Lee, K. Y.; Chung, Y. S.; Joo, J. E.; Kim, Y. H.; Oh, Ch. Y.; Lee, Y. S.; Ham, W. H. *Arch. Pharm. Res.* **2005**, *28*, 151-158. DOI: https://doi.org/10.1007/bf02977706.
25. Burgess, L. E.; Meyers, A. I.; *J. Org. Chem.* **1992**, *57*, 1656-1662. DOI: https://doi.org/10.1021/jo00032a012.
26. Overman, L. E.; Remarchuk, T. P.; *J. Am. Chem. Soc*. **2002**, *124*, 12-13. DOI: https://doi.org/10.1021/ja017198n.

J. Mex. Chem. Soc. **2024**, *68*(2)
Regular Issue

ISSN-e 2594-0317

27. Singh, V.; Saxena, R.; Batra, S. *J. Org. Chem.* **2005**, *70*, 353-356. DOI: https://doi.org/10.1021/jo048411b.
28. Sarkar, R.; Mukhopadhyay, C. *Tetrahedron Lett.* 2013, 54, 3706-3711. DOI: https://doi.org/10.1016/j.tetlet.2013.05.017.
29. Zonouz, A. M.; Eskandari, I.; Notash, B. *Synth. Commun.* **2015**, *45,* 2115-2121. DOI: https://doi.org/10.1080/00397911.2015.1065506.
30. Sun, J.; Wu, Q.; Xia, E.Y.; Yan, C. G. *Eur. J. Org. Chem.* **2011**, 2981-2986. DOI: https://doi.org/10.1002/ejoc.201100008.
31. Ahankar, H.; Ramazani, A.; Slepokura, K.; Lis, T.; Joo, S. W. *Green Chem*. **2016**, *18*, 3582-3593. DOI: https://doi.org/10.1039/c6gc00157b.
32. Marapala, K. S.; Venkatesh, N.; Swapna, M.; Venkateswar, P. R. *Int. J. ChemTech Res.* **2020**, *13*, 227-231. DOI: https://doi.org/10.20902/ijctr.2019.130128.
33. a) Pervaram, S.; Ashok, D.; Venkata Ramana Reddy, C.; Sarasija, M.; Ganesh, A. *Chem. Data Collect.* **2020**, 29, 100508. DOI: https://doi.org/10.1016/j.cdc.2020.100508. b) Ghaffari Khaligh, N.; Mihankhah, T.; Rafie Johan, M.; Titinchi, S. J. J. *Green Process Synth*. **2019**, 8, 373-381. DOI: https://doi.org/10.1515/gps-2019-0004. c) Ghaffari Khaligh, N.; Mihankhah, T.; Rafie Johan, M.; *Synth. Commun.* **2019**, *49*, 1334-1342. DOI: https://doi.org/10.1080/00397911.2019.1601225.
34. a) Ghorbani-Vaghei, R.; Sarmast, N.; Mahmoodi, J. *Appl. Organomet. Chem*. **2017**, *31*, e3681. DOI: https://doi.org/10.1002/aoc.3681. b) Esmaeilzadeh, S.; Setamdideh, D. *J. Serb. Chem. Soc.* **2021**, *86*, 1039-1056. DOI: https://doi.org/10.2298/JSC210521059E.
35. Hamdi Mohamadabad, P.; Setamdideh, D. *Org. Prep. Proced. Int.* **2023**, *55*, 265-275. DOI: https://doi.org/10.1080/00304948.2022.2141044.
36. a) Kim, H. K.; Park, J. W.; *J. Environ. Sci. Health. A.* **2019**, *54*, 648-656. DOI: https://doi.org/10.1080/10934529.2019.1579535. b) Burakevich, J. V.; Lore, A. M.; Volpp, G. P. *J. Org. Chem*. **1971**, *36*, 1-4. DOI: https://doi.org/10.1021/jo00800a001.
37. Chan, C. C. P.; Gallard, H.; Majewski, P. *J. Nanopart. Res.* **2012**, *14*, 828. DOI: https://doi.org/10.1007/s11051-012-0828-2.
38. Ebrahimi-Tazangi, F.; Hekmatara, S. H.; Yazdi, J. S. *J. Alloys Compd.* **2019**, *809*, 151779. DOI: https://doi.org/10.1016/j.jallcom.2019.151779.
39. Zhang, C. L.; Cheng, H. D.; Ren, S. Y.; Zhang, W. P.; Chen, Z.; Wang, Y.; MA, J. H.; Zhang, C. S.; Guo, Z. Y. *IOP Conf. Ser.: Earth Environ. Sci.* **2018**, *199,* 052042. DOI: https://doi.org/10.1088/1755-1315/199/5/052042.
40. Fan, G.; Rena, Y.; Jiangb, W.; Wang, C.; Xub, B.; Liu, F. *Catal. Commun.* **2014**, *52*, 22. DOI: https://doi.org/10.1016/j.catcom.2014.04.006.
41. Gao, J.; He, Y.; Zhao, X.; Ran, X.; Wuc, Y.; Su, Y.; Dai, J. *J. Colloid Interface. Sci.* **2016**, *481***,** 220-228. DOI: https://doi.org/10.1016/j.jcis.2016.07.057.
42. Chu, C.; Lu, C.; Yuan, J.; Xing, C. *Sci. Nutr.* **2020**, *8*, 3673-3681. DOI: https://doi.org/10.1002/fsn3.1651.
43. Guan, N.; Xu, J.; Wang, L.; Sun, D. *Colloid Surf. A-Phsicochem. Eng. Asp.* **2009**, *346*, 221-228. DOI: https://doi.org/10.1016/j.colsurfa.2009.06.022.
44. He, X.; Yang, W.; Li, S.; Liu, Y.; Hu, B.; Wang, T.; Hou, X. *Microchim. Acta.* **2018**, *185*, 125. DOI: https://doi.org/10.1007/s00604-018-2672-2.
45. Jafarnejad, M.; Daghighi Asli, M.; Afshar Taromi, F.; Manoochehri, M. *Int. J. Biol. Macromol.* **2020**, *148*, 201-217. DOI: https://doi.org/10.1016/j.ijbiomac.2020.01.017.
46. Lin, S.; Hua, X.; Yang, Y.; Liu, L.; Lin, K. *Water Sci. Technol.* **2017**, *76*, 452-458. DOI: https://doi.org/10.2166/wst.2017.225.
47. Das, M.; Dhak, P.; Gupta, S.; Mishra, D.; Maiti, T. K.; Basak, A.; Pramanik, P. *Nanotechnology* **2010**, *21*, 125103. DOI: https://doi.org/10.1088/0957-4484/21/12/125103.

J. Mex. Chem. Soc. **2024**, *68*(2)
Regular Issue

ISSN-e 2594-0317

48. Baghani, A. N.; Mahvi, A. H.; Gholami, M.; Delikhoon, N. R. M. *J. Environ. Health Sci. Eng.* **2016**, *14*, 11. DOI: https://doi.org/10.1186/s40201-016-0252-0.
49. Pazouki, M.; Zabihi, M.; Shayegan, J.; Fatehi, M. H. *J. Chem. Eng.* **2018**, *35*, 671-683. DOI: https://doi.org/10.1007/s11814-017-0293-9.
50. Han, L.; Li, Q.; Chen, S.; Xie, W.; Bao, W.; Chang, L.; Wang, J. *Sci. Rep.* **2017**, *7*, 7448. DOI: https://doi.org/10.1038/s41598-017-07802-8.
51. Li, Y.; Xie, Q.; Hu, Q.; Li, C.; Huang, Z.; Yang, X.; Guo, H. *Sci. Rep.* **2016**, *6,* 30651. DOI:https://doi.org/10.1038/srep30651.
52. Xiong, S.; Wang, M.; Cai, D.; Li, Y.; Gu, N.; Wu, Z.; *Anal. Lett.* **2013**, *46*, 912-922. DOI: https://doi.org/10.1080/00032719.2012.747094.
53. Tang, Z.; Li, F. *J. Comput. Theor. Nanosci.* **2016**, *13,* 772-776. DOI: https://doi.org/10.1166/jctn.2016.4873.
54. Cornell, R. M.; Schwertmann, U. U. in: *The Iron Oxides: Structure Properties, Reactions, Occurrences and Uses*, 2nd ed.; Completely Revised and Extended Edition; Wiley-VCH: Weinheim, Germany, 2003.
55. Loh, K. S.; Lee, Y. H.; Musa, A.; Salmah, A. A.; Zamri, I. *Sensors.* **2008**, *8*, 5775. DOI: https://doi.org/10.3390/s8095775.
56. Dutta, A.; Rohman, M. A.; Nongrum, R.; Thongni, A.; Mitra, S.; Nongkhlaw, R. *New J. Chem.* **2021**, *45*, 8136 -8148. DOI: https://doi.org/10.1039/D1NJ00343G.